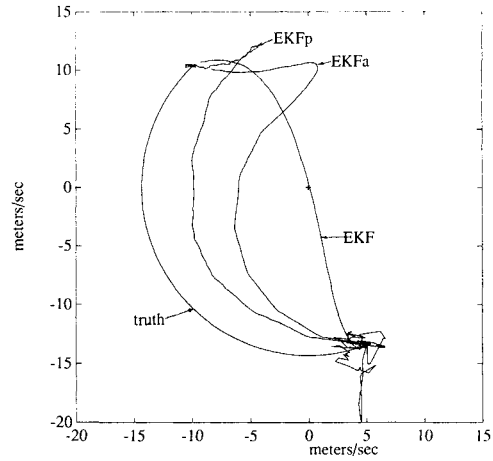

Fig. 2 Velocity performance of the filters.

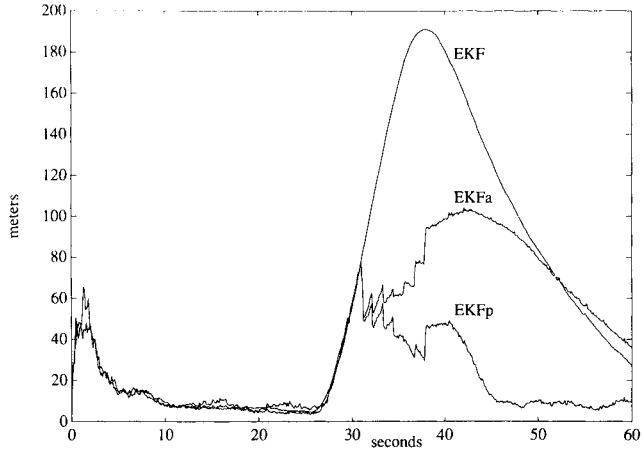

Fig. 3 Prediction performance of the filters.

incorrect references. Figure 2 shows the filter responses in the velocity plane. The EKF is notably deficient in velocity estimation, actually confusing the sense of rotation. As more of the image-derived information is incorporated into the estimate, performance improves. Covariance adaptation particularly speeds the final velocity correction after the maneuver ends.

The improved velocity estimates are reflected in prediction accuracy. Figure 3 shows the prediction responses for the same trajectory. Image-based algorithms have a noticeable local volatility due to the quantization of the orientation grid induced by the image processor. Nevertheless, it is evident that covariance adaptation speeds response. For this scenario the peak 5-s prediction error in position is 190 m, with 25 m remaining 30 s after the maneuver ends. The EKF_A reduces the peak to 110 m but has about the same residual error after 30 s. The adaptive EKF_P has a 78-m peak but only an 8-m prediction error after 15 s.

There is, of course, a penalty to be paid for the improved performance during and after a maneuver. The basic EKF was derived on the basis of a model best tuned to the nonmaneuvering target. This null EKF wastes no effort on tracking putative maneuvers, and this complacency leads to excellent nominal prediction performance, approximately a 4-m position error in quiescent null-maneuver sojourns. The adaptive filter "sees" more maneuvers than actually occur. Nevertheless, the performance deterioration is slight, in the neighborhood of 5.5 m during the same conditions. Furthermore, during an acceleration transient, prediction is so improved that the suggested modification will be useful in volative encounters.

III. Conclusions

A covariance adaptive modification of an earlier image-based tracking algorithm improves performance by increasing the filter gain during periods of uncertainty regarding the maneuver regime of the target. Since the increase in algorithmic complexity is slight, this algorithm provides a useful complement to the earlier tracker.

Acknowledgments

This research was supported by a grant from the Hughes Aircraft Co. and by the MICRO Program of the State of California under Project No. 90-158.

References

[1]Chang, C. B., and Tabaczynski, J. A., "Application of State Estimation to Target Tracking," *IEEE Transaction on Automatic Control,* Vol. AC-29, Feb. 1984, pp. 98–109.

[2]Maybeck, P. S., *Stochastic Models, Estimation, and Control,* Vol. 1, Academic Press, New York, 1979.

[3]Hutchins, R. G., and Sworder, D. D., "Image Fusion Algorithms for Tracking Maneuvering Targets," *Journal of Guidance, Control, and Dynamics* (to be published).

[4]Cloutier, J. R., Evers, J. H., and Feeler, J. J., "Assessment of Air-to-Air Missile Guidance and Control Technology," *IEEE Control, Systems Magazine,* Vol. 9, No. 4, Oct. 1989, pp. 27–34.

[5]Speyer, J. L., Kim, K. D., and Tahk, M., "Passive Homing Missile Guidance Law Based on New Target Maneuver Models," *Journal of Guidance, Control, and Dynamics,* Vol. 13, No. 5, 1990, pp. 803–812.

[6]Blom, H. A. K., and Bar-Shalom, Y., "The Interacting Multiple Model Algorithm for Systems with Markovian Switching Coefficients," *IEEE Transactions on Automatic Control,* Vol. 33, Aug. 1988, pp. 780–783.

[7]Maybeck, P. S., and Suizu, R. I., "Adaptive Tracker Field-of-View Variation Via Multiple Model Filtering," *IEEE Transactions on Aerospace and Electronic Systems,* Vol. AES-21, July 1985, pp. 529–539.

[8]Lefas, C. C., "Using Roll Angle Measurements to Track Aircraft Maneuvers," *IEEE Transactions on Aerospace and Electronic Systems,* Vol. AES-20, No. 6, Nov. 1984, pp. 671–681.

[9]Bekir, E., "Adaptive Kalman Filter for Tracking Maneuvering Targets," *Journal of Guidance, Control, and Dynamics,* Vol. 6, No. 5, 1983, pp. 414–416.

[10]Williams, D. E., and Friedland, B., "Target Maneuver Detection and Estimation," *Proceedings of the 27th IEEE Conference on Decision and Control,* Austin, TX, Dec. 1988, pp. 851–855.

[11]Sworder, D. D., and Hutchins, R. G., "Maneuver Estimation Using Measurements of Orientation," *IEEE Transactions on Aerospace and Electronic Systems,* Vol. AES-26, July 1990, pp. 626–638.

Coupling of Tether Lateral Vibration and Subsatellite Attitude Motion

S. Bergamaschi* and F. Bonon†
University of Padova, Padova 35131, Italy

Introduction

IT has long been known that the study of the motion of tethered systems in space is an intriguing problem. To be more specific, at present, after several years of effort, it seems that not every aspect of the dynamics of TSS-1 (Tethered Satellite System—Mission 1) during retrieval is adequately understood, so that, recently, actions have been taken in the United States and in Italy to increase the control capability of the system. The main simulation difficulties have been pointed out in Ref. 1, where a mixed approach, i.e., one based on

Received Jan. 3, 1991; revision received July 17, 1991; accepted for publication July 18, 1991.

*Associate Professor, Department of Mechanical Engineering, Via Venezia 1. Member AIAA.

†Research Assistant, Department of Mechanical Engineering, Via Venezia 1. Member AIAA.

several dedicated models, has been suggested for more thorough study. Simulation problems are due to a number of causes, among which is the wide spectrum of the oscillatory components of the motion. The frequencies, which, in general, depend on tether length, easily range from the mean orbital motion (2×10^{-4} Hz) to a few hertz.

Thus, if purely numerical methods are used to solve the equations of motion, the integration step must be small and the computer time needed is likely to be large. The purpose of this Note is to use a relatively simple model to study the coupling between tether taut string vibrations and satellite pendulous oscillations in the linear regime. The authors think that this problem is important for two reasons. First, in the past, in semianalytical formulations of the problem, most frequently the satellite has been considered to be a point mass, so that little is known about the ratios between tether and satellite oscillatory amplitudes and their dependence on system parameters, particularly the tether length. Second (and most important from the point of view of operations), the skip-rope problem of TSS-1 has recently pointed out the criticality of the coupling of satellite attitude dynamics with the first (or second, if rigid librations are taken into account) mode of both in-plane and out-of-plane tether vibrations. This problem has a critical practical relevance because numerical simulations have shown that the energy transfer from skip-rope to roll and pitch in the last phase of retrieval may be such that docking of the satellite to the Shuttle boom may not be feasible.

For these reasons, the numerical values adopted to obtain the results presented here are the ones pertinent to TSS-1 and particular attention will be dedicated to the half-sine deflection of the tether, in view of the amount of energy stored in it.

Mathematical Model

From the papers published by several authors (see Ref. 2 for details on the assumptions), it is known that, in the linear elastic regime, lateral out-of-plane vibrations are not coupled to longitudinal and lateral in-plane oscillations. Further, it has been shown in Ref. 3 that the coupling between extensional and taut string lateral in-plane oscillations is weak, so that one can speak of prevalently longitudinal and prevalently lateral vibration modes. In addition, the effect of the orbital mean motion n is dominant only in the pendulum-like components of the motion, whereas elasticity prevails in the higher modes, so that the frequencies of the really elastic modes of in-plane and out-of-plane lateral vibrations are almost equal and the degree of coupling with satellite motion is the same.

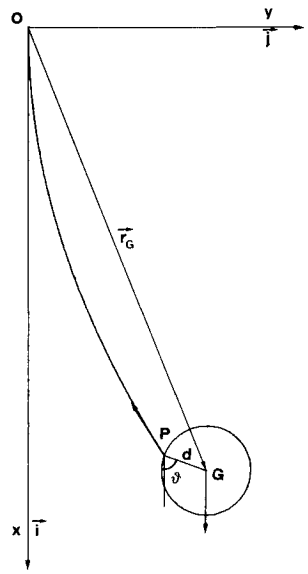

Fig. 1 Sketch of the model and meanings of the symbols used.

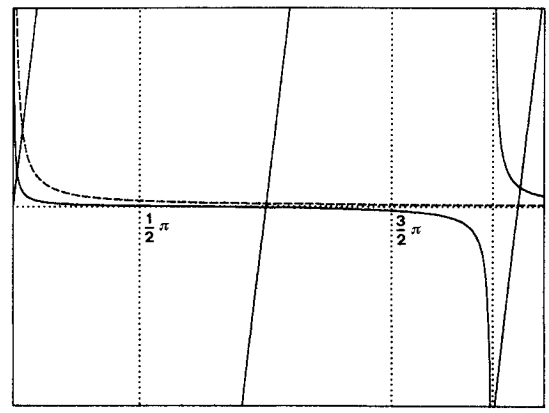

Fig. 2 Frequency equations.

Thus, the assumptions made to study the linear coupling between satellite oscillations and tether lateral vibrations are the following: 1) the motion is planar; 2) the satellite is a rigid body with inertia moment equal to I; and 3) orbital effects both on tether vibrations and satellite oscillations are negligibly small.

The meanings of some of the symbols used in the following equations are shown in Fig. 1, where x is aligned with the ascending local vertical and y is parallel to the velocity of the main body; θ is the angle between one of the principal inertia axes of the satellite (assumed to be coincident with the line joining the center of mass to the tether attachment point) and the x direction. The tether is inextensible. In virtue of the assumptions just made, the equation governing tether vibrations is

$$\ddot{y}(x,t) = (T/\mu)y''(x,t) \qquad (0 \le x \le l) \tag{1}$$

where $T = 3mn^2(l + d)$ and μ is the tether mass per unit length.

The boundary condition at $x = 0$ is

$$y(0,t) = 0 \tag{2}$$

whereas the boundary condition at l and the equation for satellite rotation are now derived by means of the Lagrange equations written in the form

$$\frac{\mathrm{d}}{\mathrm{d}t}\frac{\partial T_s}{\partial \dot{q}_i} - \frac{\partial T_s}{\partial q_i} = Q_i \qquad (i = 1,2) \tag{3}$$

where the Lagrangian coordinates are $y(l,t)$ and θ, and T_s is the kinetic energy of the satellite and the $Q_i - s$ are the generalized forces.

T_s is easily written as

$$2T_s = m\dot{r}_G \cdot \dot{r}_G + I\dot{\theta}^2$$

$$= m[\dot{y}^2(l,t) + d^2\dot{\theta}^2 + 2d\dot{y}(l,t)\dot{\theta}\cos\theta] + I\dot{\theta}^2 \tag{4}$$

The forces to be taken into account are the following:

1) The gravity-gradient force on the satellite

$$F_1 = 3mn^2(l + d\cos\theta)i \tag{5}$$

2) The tether tension at the satellite attach point

$$F_2 = -3mn^2(l + d\cos\theta)[i + y'(l,t)j] \tag{6}$$

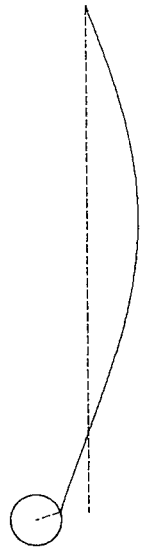

Fig. 3 Graphic representation of the modal ratio between skip-rope and satellite pendulous motion amplitude.

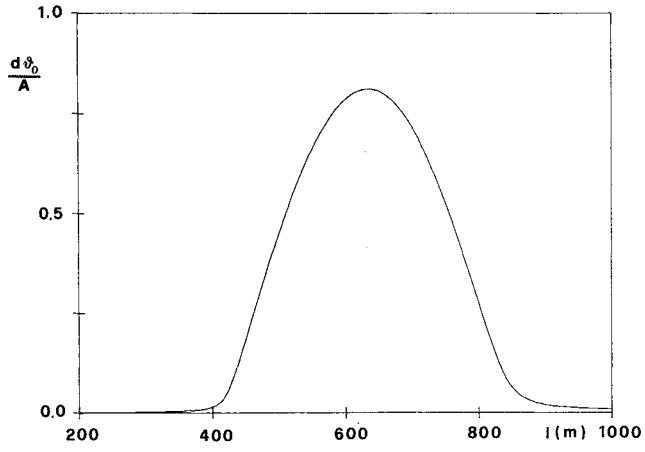

Fig. 4 Modal ratio as a function of tether length.

3) In the TSS-1 case, the in-line thrust force, if $l < 2$ km

$$F_3 = \tau(\cos\theta i + \sin\theta j) \tag{7}$$

where τ is the thrust value.

Assuming small rotation amplitudes, the boundary condition at l is written as

$$\ddot{y}(l,t) + d\ddot{\theta} + 3n^2(l+d)y'(l,t) - (\tau/m)\theta = 0 \tag{8}$$

and the rotation equation is

$$(I + md^2)\ddot{\theta} + md\ddot{y}(l,t) + 3mn^2d(l+d)\theta = 0 \tag{9}$$

Taking into account condition 2, a particular solution for $y(x,t)$ and $\theta(t)$ has the form

$$y(x,t) = Af(t)\sin\frac{\lambda x}{l}, \qquad \theta(t) = \theta_0 f(t) \tag{10}$$

where λ is the nondimensional frequency:

$$\lambda^2 = \frac{\mu l^2}{T}\omega^2 \tag{11}$$

By substituting Eqs. (10) into Eqs. (8) and (9), we can obtain the frequency equation:

$$\tan\lambda = \frac{3\mu l n^2(l+d)}{T^2\lambda}\,\frac{[(I+md^2)T\lambda^2/\mu l^2 - 3mn^2d(l+d)]}{(I\lambda^2/\mu l^2 - d)} \tag{12}$$

and the modal ratio can be written as,

$$\frac{d\theta_0}{A} = \frac{md^2T\lambda^2\sin\lambda/\mu l^2}{3mn^2d(l+d) - (I+md^2)T\lambda^2/\mu l^2} \tag{13}$$

Results and Conclusions

It is known that the classical problem of the vibrations of a taut string with one end fixed and a point mass attached to the other reduces to the solution of the frequency equation[4]:

$$\lambda\tan\lambda = \mu l/m \tag{14}$$

that is, to find the intersections between a trigonometric tangent and a hyperbola. Thus, it is interesting to compare the solutions of Eq. (14) (dashed line in Fig. 2) and of Eq. (12) (solid line) in order to evaluate the effect of the finite dimensions of the satellite.

From the structure of the equations and from Fig. 2, the following can be concluded.

1) Equation (12) admits an infinity of roots similar to the ones of Eq. (14). In fact, in both cases, their numerical values approach multiples of π as the order is increased. The corresponding amplitudes of the satellite pendulous motion are, in any case, very small.

2) In addition, Eq. (12) has a distinct, peculiar solution, caused by the second asymptote of the curve intersecting the tangent. The position of the asymptote depends on l, so that, using the parameters values pertinent to TSS-1, when the tether length is a few hundred meters, the new root is the third one and the modal shape is the one shown in Fig. 3.

The main result of this Note is shown in Fig. 4. The numerical values adopted are

$$m = 493.4 \text{ kg}, \qquad \mu = 8.35\times10^{-3} \text{ kg/m}, \qquad I = 120 \text{ kg m}^2$$

$$d = 0.8 \text{ m}, \qquad n = 1.158\times10^{-3} \text{ rad/s}$$

It is seen that the ratio $d\theta_0/A$ exhibits a bell-shaped dependence on l, with a maximum of 0.81 at $l = 630$ m. This result confirms that, if the skip-rope mode is excited during retrieval, a considerable amount of energy can be transferred to the satellite during the last phase. Additional results, not reported for sake of brevity, show that the same kind (and intensity) of coupling can be expected, at larger lengths, with the higher modes of tether lateral vibration. In these cases, however, the real amount of energy exchange is unlikely to be large because of the small amplitudes foreseen for such modes.

References

[1]Rupp, C. C., "Summary of the September 16 Tether Dynamics Simulations Workshop," Advances in the Astronautical Sciences, Vol. 62, Univelt, San Diego, CA, 1987, pp. 721-724.

[2]Bergamaschi, S., et al., "A Continuous Model for Tether Elastic Vibrations in TSS," AIAA 24th Aerospace Sciences Meeting (Reno, NV), Jan. 1986 (AIAA Paper 86-0087).

[3]Pasca, M., Pignataro, M., and Luongo, A., "Three-Dimensional Vibrations of Tethered Satellite System," *Journal of Guidance, Control, and Dynamics,* Vol. 14, No. 2, 1991, pp. 312-320.

[4]Volterra, E., and Zachmanoglou, E. C., *Dynamics of Vibrations,* Merrill, Columbus, OH, 1965, Chap. IV.